HNUE JOURNAL OF SCIENCE
Natural Sciences 2024, Volume 69, Issue 2, pp. 118-124
This paper is available online at http://hnuejs.edu.vn/ns
DOI: 10.18173/2354-1059.2024-0026

ANTI-MICROBIAL ACTIVITY OF SOME Pt(II) COMPLEXES BEARING 8-OXYQUINOLINE (8-OQ) AND EUGENOL DERIVATIVE AND 3D-STRUCTURE OF COMPLEX [PtCl(8-OQ)(EUGENOL)]

Nguyen Hoang Ninh, Dang Xuan Nhat Sang, Duong Manh Hieu and Nguyen Thi Thanh Chi*

Faculty of Chemistry, Hanoi National University of Education, Hanoi city, Vietnam

*Corresponding author: Nguyen Thi Thanh Chi, e-mail: chintt@hnue.edu.vn

Received May 30, 2024. Revised June 19, 2024. Accepted June 27, 2024.

Abstract. Four complexes including [PtCl(8-OQ)](arylolefin)] (arylolefin: Eug, **M1**; Aceug, **M2**, Eteug, **M3**, Preug, **M4**) were obtained by the reaction between 8-hydroxyquinoline and K[$PtCl_3$(arylolefin)] in high yields. The 3D structure of **M1** has been determined for the first time by DFT calculation combined with the experimental NOESY spectrum. The result showed that **M1** exists as distorted square-planar coordination with angles of O-Pt-Cl and N-Pt-O of 176.4^o and 81.0^o respectively. In which 8-OQ coordinates with Pt(II) through both the N and O atoms, Eug bonds with Pt(II) *via* the C=C_{ally} and in *trans* position to the N atom of 8-OQ. The investigation of the biological activities of the synthesized complexes showed that they display weak anti-bacterial and antifungal activities.

***Keywords*:** arylolefin, anti-microbial activities, DFT calculation, NOESY spectrum, Pt(II) complexes.

1. Introduction

Three generations of Pt-based drugs including cisplatin, oxaliplatin, and carboplatin have been used widely in chemotherapy. However, they still have some limitations in the medical clinic such as nausea, hair loss, diarrhea, and so on [1]-[4]. To overcome these limitations, many new platinum complexes with nature-derived ligands have been synthesized and showed potential for medical applications [5]-[8]. Among those, Pt(II) complexes bearing eugenol or its derivatives and 8-hydroxyquinoline (8-HOQ) such as [PtCl(8-OQ)](arylolefin)] (arylolefin: eugenol, Eug, **M1**; eugenoxyacetic acid, Aceug, **M2**; ethyl eugenol acetate, Eteug, **M3**; propyl eugenoxyacetate, Preug, **M4** exhibited potential anticancer activities [5]-[8]. For further research on anticancer mechanisms, determining the three-dimensional structure of these complexes is necessary. Single-crystal X-ray diffraction (SC-XRD) is an excellent method to confirm the 3D structure of a compound. However, this technique requires the compound as a single crystal. However, NOESY spectroscopy combined with theoretical calculations is a good

alternative solution to verify the 3D structure of compounds in cases where their single crystals are not available.

Infections caused by bacteria and fungi are among the most common complications in cancer patients due to the weakened immune system in the late stages of the disease or after radiation and chemotherapy. Therefore, it would be comprehensive to design compounds for anticancer treatment that also have potential antimicrobial and antifungal activities.

In the previous studies, the antimicrobial and antifungal activities of the complexes **M1**-**M4** have not yet been addressed. Additionally, only the 2D structure of complex **M1** has been determined [5]. In this work, the antibacterial and antifungal activities of **M1**-**M4** were evaluated. Additionally, the 3D structure of **M1** was determined by the NOESY spectrum combined with theory calculation.

2. Content

2.1. Experiments

2.1.1. Synthesis

Starting complexes K[$PtCl_3$(arylolefin)] (arylolefin: Eug, Aceug, Eteug, Preug) were synthesized as previously reported [5-8].

Complexes [PtCl(8-OQ)](arylolefin)] (arylolefin: Eug, **M1**; Aceug, **M2**, Eteug, **M3**; Preug, **M4**) were prepared according to the previous works [5]-[8] by the interaction between K[$PtCl_3$(arylolefin)] and 8-HOQ with molar ratio of 1:1 at room temperature in ethanol/water or propan-1-ol/water for **M4** with the volume ratio of 1:1. After about 3 hours, the precipitates were filtered and washed with cold ethanol or propan-1-ol for **M4**, then dried under vacuum to afford the products **M1**-**M4** with the yields of 85-93%.

2.1.2. Apparatus and methods

NOESY spectrum of **M1** was recorded on a Bruker AVANCE 500 MHz at 298–300 K in CD_3COCD_3 solvent, and the chemical shifts (δ) were internally referenced using the residual proton-solvent signals relative to tetramethylsilane.

The biological activities of **M1-M4** were tested on six types of microorganisms, including Staphylococcus aureus, Bacillus subtilis, Lactobacillus fermentum, Salmonella enterica, Escherichia coli, Pseudomonas aeruginosa, and the fungus Candida albicans at the Institute of Chemistry, Vietnam Academy of Science and Technology.

The structure of **M1** was optimized using the density functional theory (DFT) method employing the CAM-B3LYP/LANL2DZ functional/basis set. [9]. Frequency calculations were performed to confirm that the resulting structure is a ground state structure. The quantum chemical calculations were conducted using a Gaussian 09 package [10].

2.2. Result and discussion

2.2.1. Synthesis and structure of examined complexes

Complexes **M1**-**M4** were synthesized according to the reported procedures [5]-[8] in mild conditions in high yields of 85-93%. Since **M1**-**M4** were characterized by EDX,

IR, ^{1}H NMR, ^{13}C NMR spectra, NOESY spectra for **M2**, **M3**, **M4** and XRD method for **M4**. Therefore, in this study, the physical properties of those complexes were observed and used to compare (Table 1).

Table 1. Physical properties of the synthesized complexes.

Comp.	Color	Solubility			
		Water	***Ethanol***	***Acetone***	***$CHCl_3$***
M1	Yellow	Insoluble	Insoluble	Soluble	Soluble
M2	Dark Yellow	Insoluble	Insoluble	Slightly soluble	Slightly soluble
M3	Yellow	Insoluble	Slightly soluble	Soluble	Soluble
M4	Yellow	Insoluble	Slightly soluble	Slightly soluble	Soluble

The physical properties of **M1**-**M4** listed in Table 1 show the similarity to the previous reports [5]-[8]. Complex **M1** exhibited promising anticancer activity on four cancer cell lines KB, Lu-1, Hep-G2, and MCF-7 with IC_{50} values of 0.43-5.29 μM [5]. To further study this complex for the purpose of application in medical uses, the 3D structure of **M1** was elucidated by a combination of the NOESY spectrum and DFT calculation. Based on the assigned signals in the ^{1}H NMR of **M1** [5], the cross peaks in the NOESY spectrum were easily assigned. The assigned results are presented in Table 2, and the partial NOESY spectrum of **M1** is presented in Figure 1.

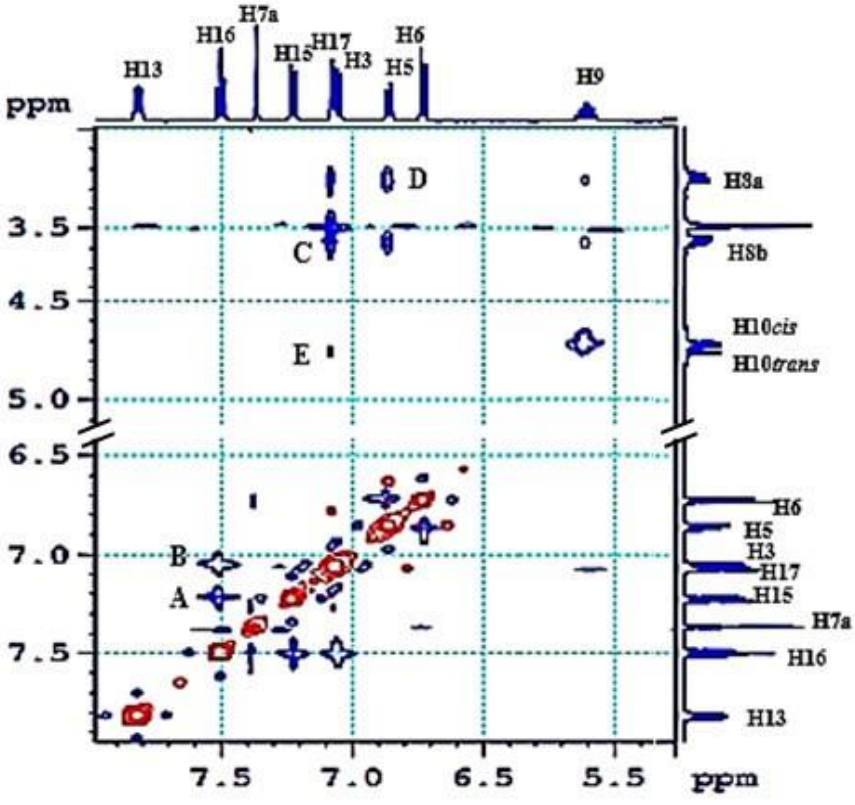

Figure 1. Partial NOESY spectrum of M1

Protons with a distance of about 2 to 4Å from each other in the space in a compound give rise to cross peaks in the NOESY spectrum of the compound [11]. For example, in the NOESY spectrum of complex **M1,** there appear A and B cross peaks corresponding to H16/H15 and H16/H17, and C and D cross peaks for H8b/H3 and H8a/H5, respectively (Figure 1). Some other cross peaks of H8a, H8b, H9, H10*cis*, and *H10trans* protons with other protons are also observed clearly in the spectrum (Table 2). Especially, there is a weak cross peak between proton H10*cis* of Eug with H17 of 8-OQ suggesting that Eug is in *trans* position to the N atom of 8-OQ in complex **M1**. To verify this conclusion, two structures ***trans*-M1** and ***cis*-M1** were optimized by DFT calculation. Both structures possess square planar coordination with the N and O atoms of 8-OQ, the C=C_{allyl} of Eug, and one Cl atom as a coordination sphere. They only differ in the relative positions of the C=C_{allyl} to the N atom/O atom. ***Trans*-M1** and ***cis*-M1** correspond to the N atom in the *trans* and *cis* position to Eug. The optimized structures of ***trans*-M1** and ***cis*-M1** are presented in Figure 2.

Table 2. Some cross peaks (ppm) in the NOESY spectrum of M1 and the selected space distances in trans-M1 determined by DFT

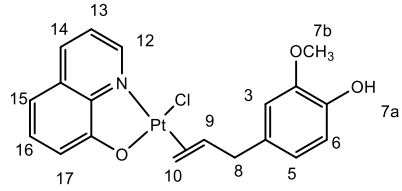

Cross peak	H/H	Cross peak	H/H	Space distance	(Å)
5.60/4.76	H9/H10*trans*	7.50/7.05	H16/H17	H3/H8b	3.757
5.60/4.71	H9/H10*cis*	4.71/7.05	H10*cis*/H17	H5/H8a	3.716
5.60/3.57	H9/H8b	7.07/3.49	H3/H7b	H17/H10*cis*	4.823
5.60/3.25	H9/H8a	7.50/7.23	H16/H15	H16/H15	2.487
4.71/3.25	H10*cis*/H8a	3.26/7.07	H8a/H3	H16/H17	2.490
4.71/3.57	H10*cis*/H8b	3.57/7.07	H8b/H3		
4.76/3.25	H10*trans*/H8a	3.25/6.85	H8a/H5		
4.76/3.57	H10*cis*/H8b	3.57/6.85	H8b/H5		

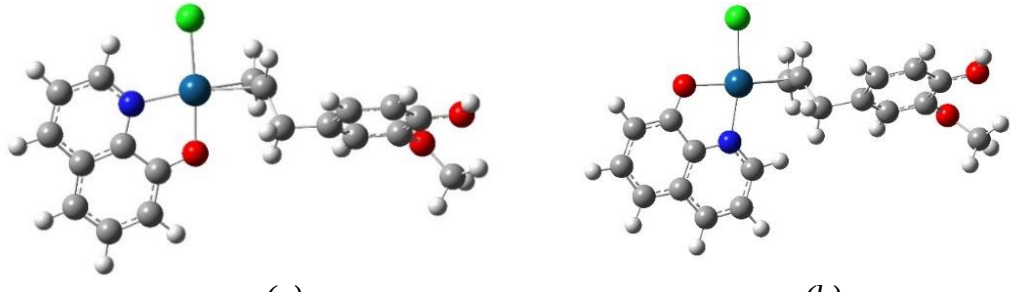

(a) *(b)*

Figure 2. The 3D calculated structures of trans-M1 (a) and cis-M1 (b)

The calculated results showed that the energy of ***cis*-M1** is 7 kcal/mole higher than ***trans*-M1**. Thereby, it could be concluded that **M1** exists in the structure ***trans*-M1**, which is consistent with the conclusion from the analysis of the NOESY spectrum above. Furthermore, some distances between protons in the space in ***trans*-M1** listed in Table 2 also show a good agreement between the cross peaks in the NOESY spectrum and the calculated distances between H-H atoms in space. Specifically, the distances from H16 to H15 and H17 of 2.487 Å and 2.490 Å, respectively result in two intensive cross peaks A and B in the NOESY spectrum of **M1** (Figure 1). Meanwhile, the longer distances such as from H3 to H8b and H5 to H8a are 3.757 Å and 3.716 Å respectively, lead to cross peaks C and D with weaker intensities. In the same way, H17 and H10*cis* give rise to a very weak cross peak E in the spectrum (Figure 1) because the space distance between them is 4.823Å.

Some selected bond lengths and angles in ***trans*-M1** as well as in **M4** and [PtCl(8-OQ)](^{i}PrEug)] (^{i}PrEug: isopropyl eugenol acetate) determined SC-XRD in previous work [8] are listed in Table 3 for comparison. The data indicate that ***trans*-M1** displays distorted square-planar coordination with bond angles of O-Pt-Cl and N-Pt-O being 176.4^o and 81.0^o respectively. The data in Table 3 show the similarity between the calculated data of ***trans*-M1** and the data of **M4** and [PtCl(8-OQ)](^{i}PrEug)]. This underscores the appropriateness of the selected computational method.

Table 3. The selected bond lengths and angles in trans-M1 determined by DFT and in M4, [PtCl(8-OQ)](^{i}PrEug)] determined by SC-XRD

Bond angle (^{o})	***trans*-M1**	**M4** [8]	**[PtCl(8-OQ)] (^{i}PrEug)]** [8]	**Bond length (Å)**	***trans*-M1**	**M4** [8]	**[PtCl(8-OQ)] (^{i}PrEug)]** [8]
N-Pt-O	81.0	82.9	82.4	Pt-N	2.088	2.042	2.039
O-Pt-Cl	176.4	177.0	176.7	Pt-O	2.049	2.003	2.014
N-Pt-Cl	95.5	94.6	94.7	Pt-Cl	2.338	2.294	2.295
N-Pt-C9	159.1	154.4	153.7	Pt-C9	2.201	2.174	2.134
N-Pt-C10	161.4	166.3	166.1	Pt-C10	2.157	2.136	2.172

Taken together, the findings above indicate that **M1** possesses the 3D structure as presented in Figure 2a.

2.2.2. In vitro cytotoxicity

Complexes **M1**-**M4** were tested *in vitro* activity against 6 types of microorganisms including *L. fermentum, B. subtilis, S. aureus, S. enterica, E. coli, P. aeruginosa,* and *C. albicans* fungus. The result is listed in Table 4.

Table 4. The result of the anti-microbial activity of examined compounds

Comp.	**The half-maximal inhibitory concentration (IC50: µg/mL)**						
	Gram (+)			***Gram (-)***			***Fungus***
	S. aureus	*B. subtilis*	*L. fermentum*	*S. enterica*	*E.coli*	*P. aeruginosa*	*C. albican*
M1	>128	>128	>128	>128	>128	>128	>128
M2	>128	96.25	>128	>128	>128	>128	>128
M3	>128	>128	>128	>128	>128	>128	>128
M4	>128	>128	>128	>128	>128	>128	>128

The results in Table 4 show that **M1**-**M4** exhibited poor antibacterial and antifungal activities on all tested bacteria and *C. albicans* fungus. Only **M2** has weak activity against *B. subtilis* with IC_{50} of 96.25 μg/mL. The weak activity against microorganisms and fungi was also observed in our previous study for another complex of Pt(II) bearing Eteug and morpholine [12]. These findings provide insight for future research that we should not focus on exploring the anti-microbial activity of platinum(II) complexes containing aryl olefins and heterocyclic amines such as 8-OQ.

3. Conclusions

In this study, by the reaction between K[$PtCl_3$(arylolefin)] and 8-hydroxyquinoline, four complexes including [PtCl(8-OQ)](arylolefin)] (arylolefin: Eug, **M1**; Aceug, **M2**, Eteug, **M3**, Preug, **M4**) were synthesized in high yields of 85-93%.

The 3D structure of **M1** was determined using the NOESY spectrum and DFT calculations for the first time. The computational and compared experimental values indicated that **M1** exists in a distorted square planar structure with bond angles of O-Pt-Cl and N-Pt-O being 176.4^o and 81.0^o respectively, which is similar to the structure of **M4** determined by SC-XRD. The center Pt(II) atom is surrounded by one Cl atom, the N and O atoms of 8-OQ, the C=C bond of Eug with the C=C bond, and the O atom is in *cis* position with each other.

The investigation of bio-activities showed that **M1**-**M4** had weak antibacterial and antifungal activities. This indicates that Pt(II) complexes containing arylolefin and 8-hydroxylquinoline should be only focused on studying anticancer activity other than on antibacterial and antifungal activities.

Acknowledgements. The authors would like to thank Dr. Tran Ngoc Dung for his assistance in DFT theoretical calculation in this work.

REFERENCES

[1] Johnstone TC, Suntharalingam K, & Lippard SJ, (2016). The next generation of platinum drugs: targeted Pt (II) agents, nanoparticle delivery, and Pt (IV) prodrugs. *Chemical Reviews*, 116(5), 3436-3486.

[2] Parveen S, (2022). Platinum-based cancer chemotherapeutics: Recent trends and future perspectives. Current Chinese Science, 2(4), 275-293.

[3] Qi J, Zheng Y, Li B, Wei L, Li J, Xu X & Wang Y, (2022). Mechanism of vitamin B6 benzoyl hydrazone platinum (II) complexes overcomes multidrug resistance in lung cancer. *European Journal of Medicinal Chemistry*, 237, 114415.

[4] Kantoury M, Eslami Moghadam M, Tarlani AA, & Divsalar A, (2016). Structure effect of some new anticancer Pt (II) complexes of amino acid derivatives with small branched or linear hydrocarbon chains on their DNA interaction. *Chemical Biology & Drug Design*, 88(1), 76-87.

[5] Nguyen TTC, Tran TD, Nguyen VH & Nguyen HD, (2017). Synthesis and spectral characterization of platinum (II) complexes containing eugenol, a natural allylphenol. *Journal of Coordination Chemistry*, 70(6), 1008-1019.

[6] Nguyen TMH, Nguyen TH, Truong TCM & Nguyen TTC, (2016). Synthesis, structure, anti-tumour activities of two platinum(ii) complexes bearing methyleugenol and p-chloroaniline. *Vietnam Journal of Chemistry*, 54(5), 549 (in Vietnamese).

[7] Nguyen TTC, Tran TD, (2014). Synthesis, structure, and biological activity of three platinum (II) complexes bearing alkyleugenoxyacetate (alkyl: ethyl or propyl) and heterocyclic amine. *Vietnam Journal of Chemistry*, 52(2), 256.

[8] Nguyen TTC, Pham VT, Truong TCM, Meervelt LV, (2018). Mixed natural arylolefin–quinoline platinum(II) complexes: synthesis, structural characterization and in vitro cytotoxicity studies. *Acta Crystallographica. Section C, Structural Chemistry*, 74(12), 1732-1743.

[9] Yanai T, Tew DP, & Handy NC, (2004). A new hybrid exchange–correlation functional using the Coulomb-attenuating method (CAM-B3LYP). *Chemical Physics Letters*, 393(1-3), 51-57.

[10] Frisch MJEA, (2009). Gaussian 09, Revision d. 01, Gaussian. *Inc, Wallingford CT*, 201.

[11] Noggle J, (2012). *The nuclear Overhauser effect*. Elsevier.

[12] Nguyen TTC, Nguyen TMH, Truong TCM, (2016). Anti-microbial activities of two platinum(II) complexes bearing ethyl eugenol acetate and synthesis, the structure of [PtCl(ethyl eugenoxyacetate-1H)(morpholine)]. *HNUE Journal of Science*, 61*(9),* 60-67.